EGFR Inhibition in Glioma Cells Modulates Rho Signaling to Inhibit Cell Motility and Invasion and Cooperates with Temozolomide to Reduce Cell Growth

Guillem Ramis[1], Elena Thomàs-Moyà[1], Silvia Fernández de Mattos[1,2], José Rodríguez[1¤], Priam Villalonga[1,2]*

1 Cancer Cell Biology Group, Institut Universitari d'Investigació en Ciències de la Salut (IUNICS), Universitat de les Illes Balears, Illes Balears, Spain, 2 Departament de Biologia Fonamental, Universitat de les Illes Balears, Illes Balears, Spain

Abstract

Enforced EGFR activation upon gene amplification and/or mutation is a common hallmark of malignant glioma. Small molecule EGFR tyrosine kinase inhibitors, such as erlotinib (Tarceva), have shown some activity in a subset of glioma patients in recent trials, although the reported data on the cellular basis of glioma cell responsiveness to these compounds have been contradictory. Here we have used a panel of human glioma cell lines, including cells with amplified or mutant EGFR, to further characterize the cellular effects of EGFR inhibition with erlotinib. Dose-response and cellular growth assays indicate that erlotinib reduces cell proliferation in all tested cell lines without inducing cytotoxic effects. Flow cytometric analyses confirm that EGFR inhibition does not induce apoptosis in glioma cells, leading to cell cycle arrest in G_1. Interestingly, erlotinib also prevents spontaneous multicellular tumour spheroid growth in U87MG cells and cooperates with sub-optimal doses of temozolomide (TMZ) to reduce multicellular tumour spheroid growth. This cooperation appears to be schedule-dependent, since pre-treatment with erlotinib protects against TMZ-induced cytotoxicity whereas concomitant treatment results in a cooperative effect. Cell cycle arrest in erlotinib-treated cells is associated with an inhibition of ERK and Akt signaling, resulting in cyclin D1 downregulation, an increase in $p27^{kip1}$ levels and pRB hypophosphorylation. Interestingly, EGFR inhibition also perturbs Rho GTPase signaling and cellular morphology, leading to Rho/ROCK-dependent formation of actin stress fibres and the inhibition of glioma cell motility and invasion.

Introduction

Malignant gliomas constitute the most common primary brain tumours in adults and rank among the most devastating and aggressive types of human cancer due to their dismal prognosis. Key biological features of these tumours are the ability of tumour cells to invade healthy brain tissue and their enhanced resistance to radio and chemotherapy-induced apoptosis [1]. Such characteristics have dramatic clinical consequences, since they critically challenge the success of therapeutic intervention. A number of genetic alterations are responsible for the malignancy of these tumours, often involving mutations leading to the hyperactivation of receptor tyrosine kinases. Among these, the epidermal growth factor (EGF) receptor (EGFR) is commonly overexpressed and amplified in gliomas, and contributes to uncontrolled proliferation and survival of glioma cells [2]. The EGFR is also frequently mutated in these tumours, leading to the expression of a truncated receptor termed EGFRvIII which lacks its extracellular domain and is constitutively active [3,4]. Enhanced activation of the EGFR tyrosine kinase domain leads to the activation of in-

tracellular signaling pathways such as the Raf/MEK/ERK and the PI3K/Akt pathways, which are ultimately responsible for the malignant phenotype of glioma cells. Accordingly, small molecule inhibitors of EGFR such as erlotinib (Tarceva) and gefitinib (Iressa) have been shown to attenuate glioma cell proliferation *in vitro* [5–7], although their clinical activity as single agents remains controversial due to the contradictory data obtained in clinical trials (reviewed in [8]). Similarly, opposing results have been reported regarding the predictive value of different biomarkers such as EGFR and EGFRvIII expression on EGFR inhibitor responsiveness. For instance, it has been described that sensitivity to erlotinib correlates with high EGFR expression levels but not with EGFRvIII expression [9] and, oppositely, that EGFRvIII expression correlates with sensitivity to erlotinib, whereas EGFR expression does not [6]. In contrast, it is well-established that sensitivity to EGFR inhibition correlates with low PI3K/Akt activity, since hyperactivation of the PI3K/Akt pathway through phosphatase and tensin homolog (PTEN) mutation renders glioma cells resistant to EGFR inhibition and, conversely, inhibition of

PI3K signaling using different compounds has been shown to sensitize glioma cells to EGFR inhibitors [6,9–11]. Altogether, despite the research efforts focused on understanding the molecular basis of sensitivity to EGFR inhibitors, the prevailing view is that an in-depth analysis of the molecular responses elicited by these compounds in glioma cells is still required. Here we have aimed to further characterize the cellular effects of EGFR inhibition with erlotinib in a panel of human glioma cell lines. Erlotinib treatment reduces cell growth and inhibits multicellular tumour spheroid formation. These effects are accompanied by alterations in signaling pathways and cell cycle regulators. Interestingly, EGFR inhibition can cooperate in a schedule-dependent manner with low doses of temozolomide (TMZ) to reduce glioma cell growth. We also show that EGFR inhibition induces a dramatic alteration in cell morphology through the modulation of Rho/ROCK signaling that leads to the inhibition of glioma cell motility and invasion. Importantly, EGFR inhibition is similarly effective in the reduction of proliferation, motility and invasion in cells expressing wild-type, mutant or amplified EGFR.

Materials and Methods

Cell culture and drug treatments

LN229, U87MG, HS683, T98G, U251 and U373 cells were a gift from Joan Seoane (Institut de Recerca Hospital Universitari Vall d'Hebron, Barcelona). The U87MG derivative cell line U87ΔEGFR was a gift from Isabel Martínez-Lacaci (Hospital Universitario Virgen de la Arrixaca, Murcia). SKMG-3 cells were a gift of Hans Skovgaard (Rigshospitalet, Oslo). All cell lines were subconfluently grown and passaged, routinely tested for myco-plasma contamination and subjected to frequent morphological tests and growth curve analysis as quality-control assessments. Cells were grown in DMEM (Invitrogen, Carlsbad, CA) supplemented with 10% foetal calf serum (Biological Industries, Israel) in a humidified incubator at 37°C with 5% CO2. Erlotinib (Roche, Basel, Switzerland), temozolomide (Developmental Therapeutics Program, Division of Cancer Treatment and Diagnosis, National Cancer Institute, Bethesda, MA), C3 (Cytoskeleton, Denver, CO) and H-1152 (Calbiochem, Darmstadt, Germany) were added directly to the media at the indicated concentration and cells were harvested or analyzed at the time points indicated in the figure legends.

Measurement of cell proliferation and viability

For cellular growth assays, 2.5×10^4 cells were plated in 6-well plates and cell growth was assessed at the indicated time points counting cells after trypsinizing and incubating them with trypan blue solution (Sigma-Aldrich, St. Louis, MO). For cellular viability assays, 5×10^3 cells were plated in clear bottom 96-well plates, treated as indicated and processed using the CellTiter-Glo Luminiscent Assay Kit (Promega, Madison, WI) to measure cellular viability, following the manufacturer's instructions. Luminiscence was detected using a multiwell scanning spectro-photometer (Plate Chameleon, Hidex, Finland).

Multicellular tumour spheroid formation assays

To monitor the formation of multicellular tumour spheroids in culture, 4×10^5 U87MG cells were plated in 6-well plates and treated as indicated in the figure legends. After 4–6 days cells were stained with 0.5% (w/v) crystal violet in 70% ethanol and the number of multicellular tumour spheroids from representative fields (>10) counted under a light microscope.

Flow Cytometry

Cell cycle profile was measured by flow cytometry using propidium iodide. Briefly, trypsinized cells were collected by centrifugation, washed in PBS and fixed for 30 min at 4°C in 70% ethanol. After washing twice with PBS, DNA was stained with 50 μg/ml propidium iodide (Sigma-Aldrich, St. Louis, MO) in the presence of 50 μg/ml RNase A (Sigma-Aldrich, St. Louis, MO). Stained cells were then processed using a Beckman Coulter EPICS XL Cytometer (Beckman Coulter, Fullerton, CA) and analyzed with the WinMDI software.

Clonogenic assays

For clonogenic assays, cells grown in 6-well plates were treated as indicated, trypsinized and plated at low density (3×10^3 cells per 60-mm plate) in fresh media. After 7–10 days cells were stained with 0.5% (w/v) crystal violet in 70% ethanol and the number of colonies counted.

Actin Staining

Cells grown on coverslips were fixed in 3.7% (v/v) para-formaldehyde for 20 min and permeabilized in 0.1% (v/v) Triton X-100 for 5 min. Actin filaments were visualized by incubating the fixed cells for 45 min at 37°C with TRITC-phalloidin (Sigma-Aldrich, St. Louis, MO, 1:500). Stained cells were analyzed on a Leica TCS SPE confocal microscope (Leica Microsystems, Wetzlar, Germany).

Measurement of Rho GTPase activity

The capacity of Rho-GTP and Rac-GTP to bind to GST-Rhotekin and GST-PBD (p21-activated-kinase-binding-domain) respectively was used in order to analyze the amount of active GTPases [12] with Rho and Rac activation assay kits (Cytoskel-eton, Denver, CO), according to the manufacturer's instructions. Briefly, cells ($5–10 \times 10^6$) were lysed, cleared ($10,000 \times g$) and incubated for 45 min at 4°C with glutathione sepharose-4B beads coupled with GST-Rhotekin or GST-PBD for Rho-GTP or Rac-GTP pulldowns, respectively. Beads were washed 4 times in Lysis Buffer. Bound proteins were solubilized by the addition of 35 μl of Laemmli loading buffer and separated on 12.5% SDS-polyacri-lamide gels. The amount of Rho or Rac in the bound fraction was detected by western blotting.

Motility and invasion assays

For 2D motility (wound-healing) assays, 4×10^5 U87MG cells were plated in 6-well plates, wounded thrice with a sterile tip and 3 representative images were collected. After 16 h, images of the same regions were collected and the ratio of cell motility in each experimental condition quantified. For 3D invasion assays, 2×10^4 U87MG cells were seeded on matrigel-coated transwells (BD Biosciences, San Diego, CA) containing DMEM supplemented with 0.5% FCS and placed in 24-well plates containing DMEM supplemented with 10% FCS to create a growth factor gradient. 24 h later, the matrigel layer was removed and cells were stained with 0.5% (w/v) crystal violet in 70% ethanol. Invading cells from 6 representative fields were counted under a light optic micro-scope.

Gel electrophoresis and immunoblotting

Cells were harvested in a buffer containing 50 mM Tris-HCl pH 7.4, 150 mM NaCl, 1 mM EDTA and 1% (v/v) Triton X-100 plus protease and phosphatase inhibitors. Protein content was measured by the Bradford procedure [13]. Cell lysates were electrophoresed in SDS-polyacrylamide gels. After electrophoresis
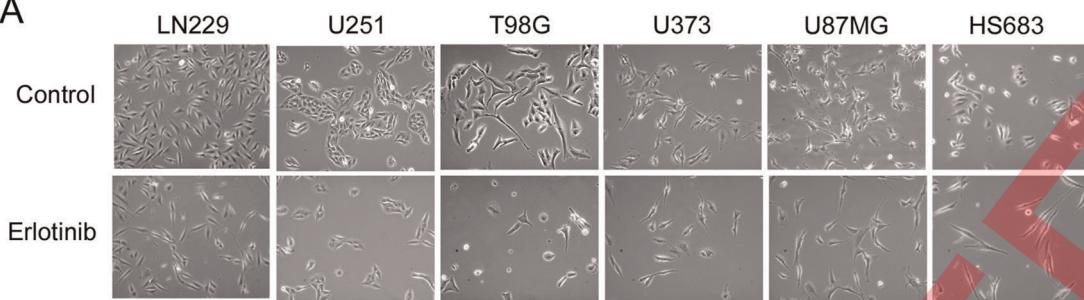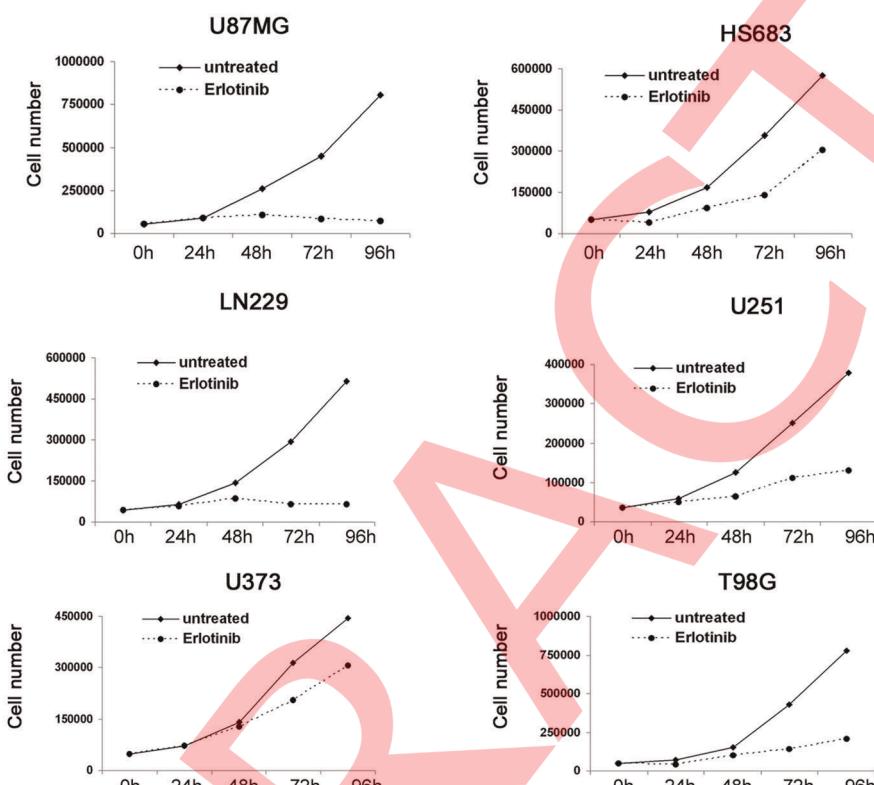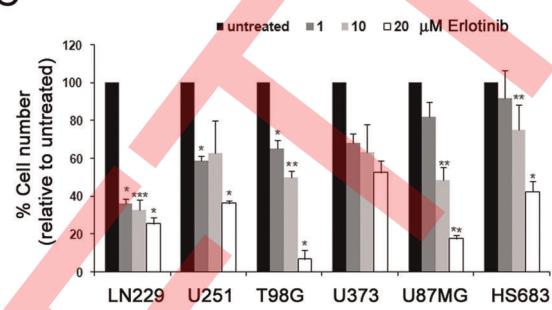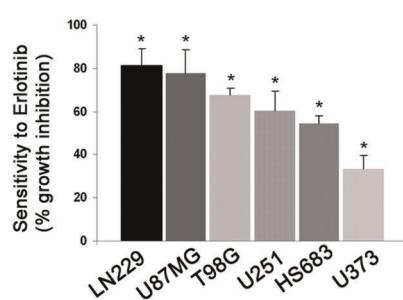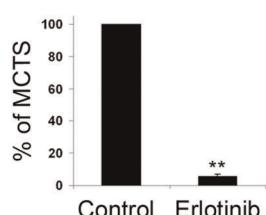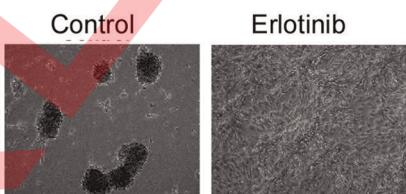
Figure 1. Erlotinib inhibits glioma cell proliferation. (A) Representative phase-contrast micrographs of glioma cell lines left untreated (control) or treated for 48 h with 10 µM erlotinib (erlotinib). (B) Glioma cell lines were left untreated (untreated) or treated with 10 µM erlotinib (erlotinib) and the number of cells counted every 24 h. Data from a representative experiment out of three repetitions is shown, representing the total number of viable cells in untreated and erlotinib-treated conditions at the indicated time-points. (C) Glioma cell lines were treated for 72 h with the indicated concentrations of erlotinib. The mean $\pm$ SD values from three independent experiments, each conducted in duplicate, are shown in the graph, representing the percentage of viable cells relative to untreated conditions. The differences between control and erlotinib treatment are statistically significant (Student's t-test: *$P<0.05$, **$P<0.01$ and ***$P<0.001$, respectively). (D) Glioma cell lines were treated for 72 h with 10 µM erlotinib. Sensitivity to erlotinib of each cell line is expressed as the mean $\pm$ SD percentage of growth inhibitory activity from three independent experiments, each conducted in duplicate. The differences between control and erlotinib treatment are statistically significant (Student's t-test: *$P<0.05$) (E) Representative phase-contrast micrographs of U87MG cells left for 4–6 days to allow formation of multicellular tumour spheroids (MCTS), untreated (control) or treated with 10 µM erlotinib (erlotinib). The graph indicates the mean $\pm$ SD values of MCTS formation from three independent experiments, each conducted in duplicate, expressed as the percentage of MCTS relative to untreated cells. The differences between control and erlotinib treatment are statistically significant (Student's t-test: **$P<0.01$).
doi:10.1371/journal.pone.0038770.g001

the proteins were transferred to Immobilon-P strips (Millipore, Billerica, MA) for 2 h at 60 V. The sheets were preincubated in TBS (20 mM Tris-HCl pH 7.5, 150 mM NaCl), 0.05% Tween 20 and 5% defatted milk powder for 1 h at room temperature and then incubated for 1 h at room temperature in TBS, 0.05% Tween 20, 1% BSA and 0.5% defatted milk powder containing the appropriate antibodies: Akt (sc-1618, 1:1000), p27^{kip1} (sc-525, 1:1000), cdk4 (sc-260, 1:1000) and p21^{cip1} (sc-471, 1:1000) from Santa Cruz (Santa Cruz, CA), anti-cyclin D1 (MS-210P, Neomarkers, Fremont, CA 1:1000), pRB (14001A, BD-Pharmingen, San Diego, CA, 1:500), Rho (ARH03, Cytoskeleton, Denver, CO, 1:500), Rac (05–389, Millipore, Billerica, MA, 1:1000), anti-β-tubulin (T0198, Sigma-Aldrich, St. Louis, MO, 1:4000) and EGFR (#2232, 1:1000), p-S473-Akt (#9271, 1:500), p-ERK (#9101, 1:1000) and ERK (#9102, 1:1000) from Cell Signaling (Beverly, MA). After washing in TBS, 0.05% Tween 20, the sheets were incubated with a peroxidase-coupled secondary antibody (Dako, Glostrup, Denmark, 1/2000 dilution,) for 1 h at room temperature. After incubation, the sheets were washed twice in TBS, 0.05% Tween 20 and once in TBS. The peroxidase reaction was visualized by the enhanced chemiluminiscence detection system (Millipore, Billerica, MA).

Statistical analysis

The statistical significance of differences was assessed by Student's t test using GraphPad Prism (GraphPad Software Inc. La Jolla, CA). Statistically significant differences are indicated by ***$p<0.001$, **$p<0.01$ and *$p<0.05$.

Results

Erlotinib inhibits glioma cell proliferation and prevents multicellular tumour spheroid formation

In order to characterize the cellular effects of EGFR inhibition in glioma cells, we treated a panel of 6 human glioma cell lines (LN229, U87MG, HS683, T98G, U251, U373) with erlotinib. Erlotinib reduced cell proliferation in all cell lines tested (Figures 1A, 1B). Growth curve experiments upon long-term erlotinib treatment indicated that erlotinib decreased total cell number (Figure 1B), but did not affect cellular viability as indicated by trypan blue staining (data not shown). Dose-response experiments confirmed that 10 µM erlotinib exerted an inhibitory effect on glioma cell growth ranging from 30% (U373 cells) to 80% inhibition (LN229 cells) (Figures 1C, 1D). Since U87MG cells spontaneously form multicellular tumour spheroids in culture [14], we also investigated whether erlotinib could prevent multicellular tumour spheroid formation. Whereas control U87MG cells formed high numbers of large and dense multicellular tumour spheroids, erlotinib-treated cells were largely resistant to spheroid

formation (Figures 1E). These observations confirm that EGFR inhibition with erlotinib severely reduces glioma cell proliferation.

Erlotinib induces G$_1$ phase arrest in glioma cells

In order to characterize the cell cycle arrest induced by erlotinib treatment in glioma cells, we performed flow cytometric analysis in a panel of control and erlotinib-treated glioma cell lines. Erlotinib treatment led to a significant accumulation of cells in G$_1$ in all tested cell lines (Figure 2A), showing a sensitivity to erlotinib in correlation with our previous results (Figure 2B). Interestingly, erlotinib did not induce cell death as indicated by the absence of a detectable sub-G$_1$ population (Figures 2A and 2B), in line with our previous data. Altogether, our results indicate that erlotinib inhibits glioma cell proliferation primarily by inhibiting S-phase entry.

EGFR inhibition cooperates with temozolomide to inhibit glioma cell growth

The current therapy for glioma patients involves the use of the alkylating agent temozolomide (TMZ) in combination with radiotherapy. We therefore investigated whether erlotinib could potentiate the antiproliferative effects of TMZ in glioma cells. For this purpose we used different experimental strategies. First, we performed clonogenic assays upon TMZ treatment of control or erlotinib-treated cells to assess if EGFR inhibition could potentiate TMZ-induced genotoxicity. LN229, U251 and HS683 cells pre-treated for 24 h with erlotinib recovered some of their clonogenic ability when re-plated in the absence of erlotinib (Figure 3A). In contrast, a short exposure to TMZ (3 h) dramatically compromised their clonogenic capacity (Figure 3A). Interestingly, erlotinib pre-treatment protected cells from TMZ-induced genotoxicity (Figure 3A). To extend these observations, we next monitored cell proliferation in MTT-based assays. In order to test whether erlotinib could cooperate with TMZ we used sub-optimal doses of both erlotinib (1 µM) and TMZ (25 µM). As expected, neither erlotinib nor TMZ at sub-optimal doses were able to significantly reduce cellular growth (Figure 3B). However, when used in combination, erlotinib was able to cooperate with TMZ to reduce cell proliferation in both U87MG and U251 cells (Figure 3B). In order to validate these results, we performed multicellular tumour spheroid formation assays using U87MG cells. To this end, U87MG cells were treated with sub-optimal doses of erlotinib (1 µM) and TMZ (25 µM), alone or in combination, and the formation of multicellular tumour spheroids was assessed. Similarly to control cells, cells treated with sub-optimal doses of erlotinib or TMZ alone gave rise to a high number of spheroids (Figures 3C). In sharp contrast, the combination of sub-optimal doses of erlotinib and TMZ dramatically reduced spheroid formation, similarly to the standard erlotinib treatment (Figures 3C). These results suggest that the combination of low

A
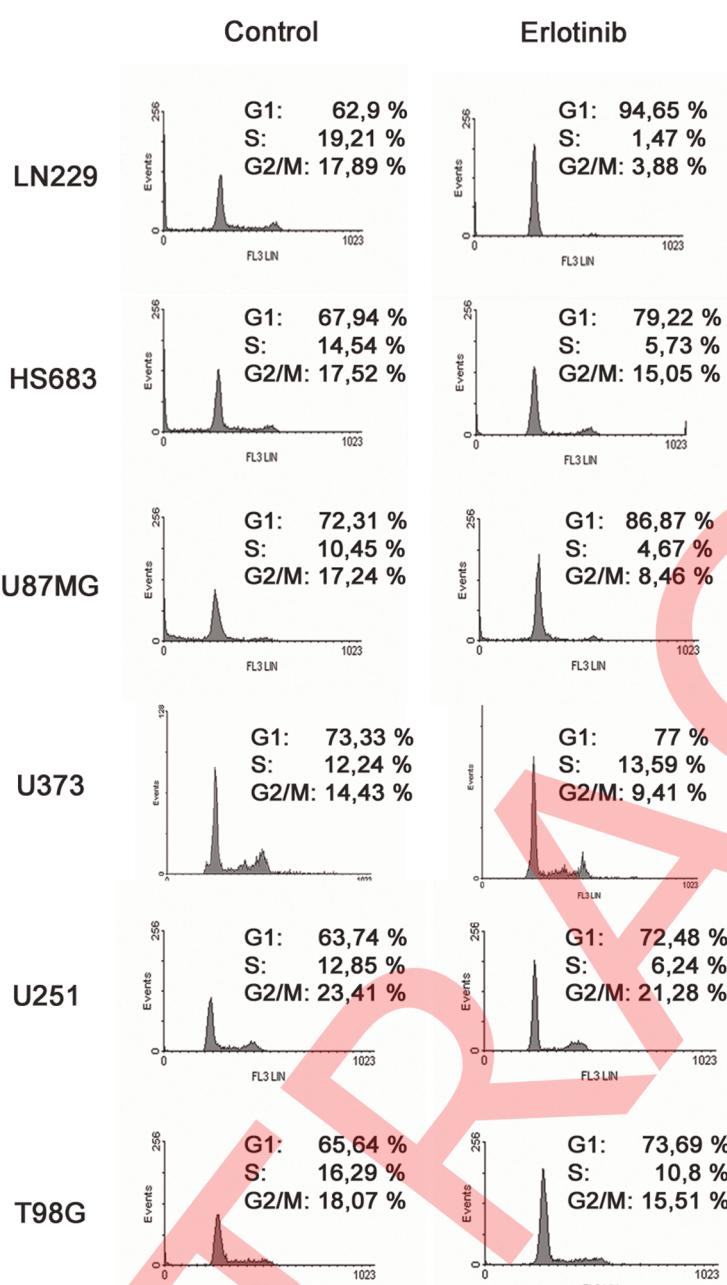
B
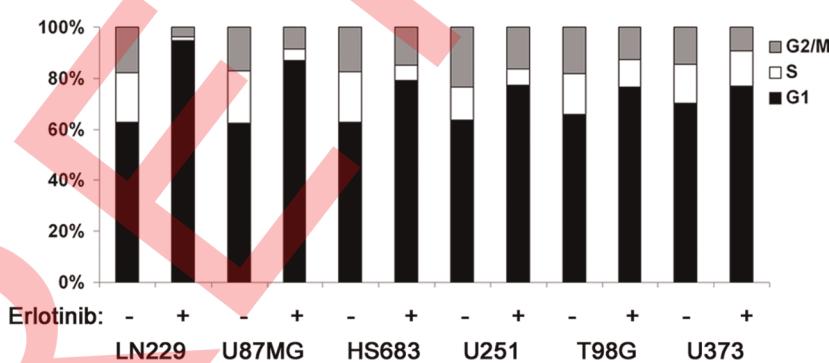
Figure 2. Erlotinib prevents multicellular tumour spheroid formation and induces G_1 arrest in glioma cells. (A) Glioma cell lines were left untreated (control) or were treated for 24 h with 10 µM erlotinib (erlotinib). Cells were harvested and their DNA content analyzed by flow

cytometry as described in Materials and Methods. The cell cycle distribution is shown for each experimental condition. (B) The graph summarizes the flow cytometry data obtained in all glioma cell lines, indicating the cell cycle distribution in control and 24 h erlotinib-treated conditions for each cell line.
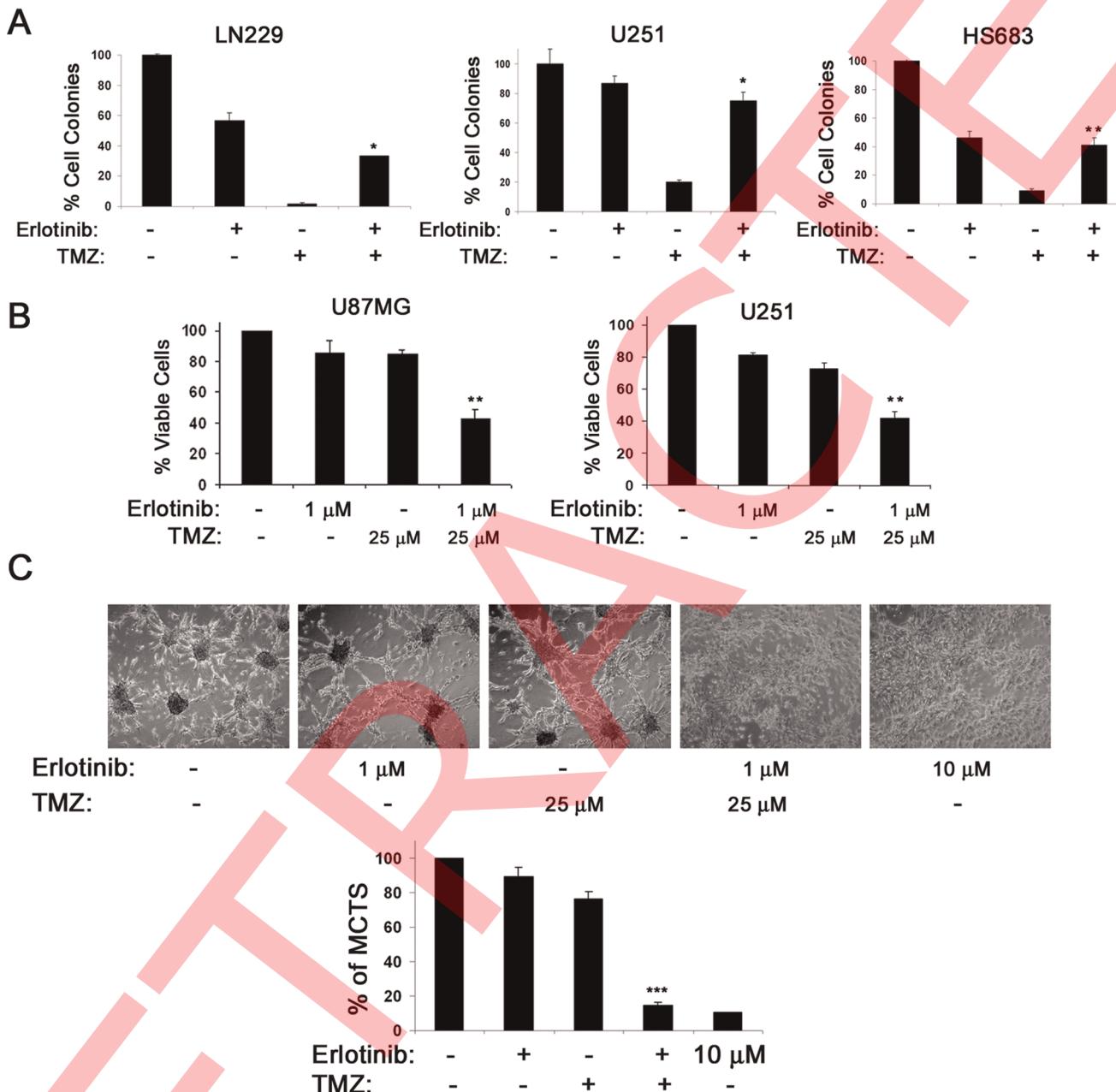
Figure 3. EGFR inhibition cooperates with temozolomide to inhibit glioma cell growth. (A) LN229, U251 and HS683 cells were left untreated or were treated for 24 h with erlotinib and subsequently exposed to vehicle or TMZ for 3 h, plated and after 7–10 days the remaining colonies were stained and counted as indicated in Materials and Methods. The mean ± SD values from three independent experiments, each conducted in duplicate, are shown in the graph, representing the number of clones relative to untreated cells. The differences between combined treatment and either treatment alone are statistically significant (Student's t-test: *P<0.05 and **P<0.01, respectively). (B) U251 and U87MG cells were plated in 96-well plates, left untreated or treated as indicated for 48 h and cell viability monitored as described in Materials and Methods. The mean ± SD values from three independent experiments, each conducted in duplicate, are shown in the graph, representing the percentage of viable cells relative to untreated cells. The differences between combined treatment and either treatment alone are statistically significant (Student's t-test: **P<0.01). (C) Representative phase-contrast micrographs of U87MG cells treated as indicated and left for 4–6 days to allow formation of MCTS. The graph indicates the mean ± SD values of MCTS formation from three independent experiments, each conducted in duplicate, expressed as the percentage of MCTS relative to untreated cells. The differences between combined treatment and either treatment alone are statistically significant (Student's t-test: ***P<0.001).
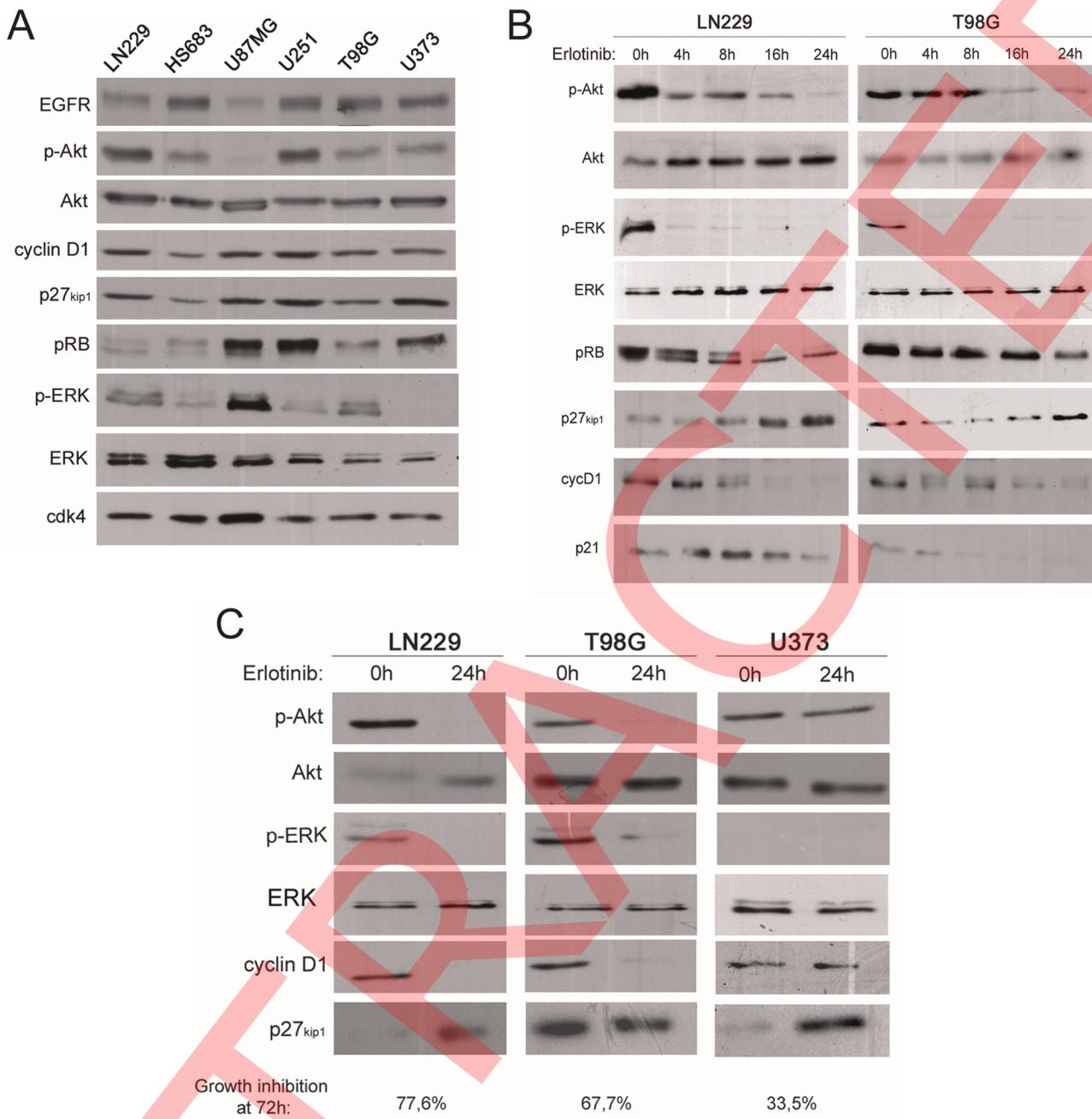
Figure 4. EGFR inhibition alters the expression levels of key cell cycle regulators. (A) The indicated human glioma cell lines were harvested and the expression levels of the indicated proteins were analyzed by western blotting with specific antibodies. (B) LN229 and T98G cells were treated with 10 µM erlotinib for the indicated time, harvested and the expression levels of the indicated proteins were analyzed by western blotting with specific antibodies. (C) As in B, but LN229, T98G and U373 cells were treated as indicated.
doi:10.1371/journal.pone.0038770.g004

doses of erlotinib and TMZ can cooperate to reduce glioma cell proliferation.

Erlotinib inhibits ERK and Akt signaling promoting cyclin D1 downregulation and increasing p27^{kip1} levels

We next investigated the molecular mechanisms responsible for the cell cycle arrest induced by EGFR inhibition, monitoring alterations on relevant signaling intermediates and cell cycle regulatory proteins in glioma cells (Figure 4A). For this purpose we performed a time-course experiment upon erlotinib treatment in LN229 and T98G cells. Erlotinib induced a rapid inhibition of ERK phosphorylation and an inhibition of Akt phosphorylation that was apparent upon longer term treatment (Figure 4B). Erlotinib also induced a significant downregulation of cyclin D1 and similarly reduced the levels of p21^{cip1} (Figure 4B). In contrast, Erlotinib increased the levels of the cyclin-dependent kinase inhibitor p27^{kip1} (Figure 4B). In agreement with these observations, erlotinib inhibited pRb phosphorylation (Figure 4B). We next investigated whether the observed molecular events correlated with the sensitivity to erlotinib in different glioma cell lines. To this end, we compared the aforementioned molecular alterations
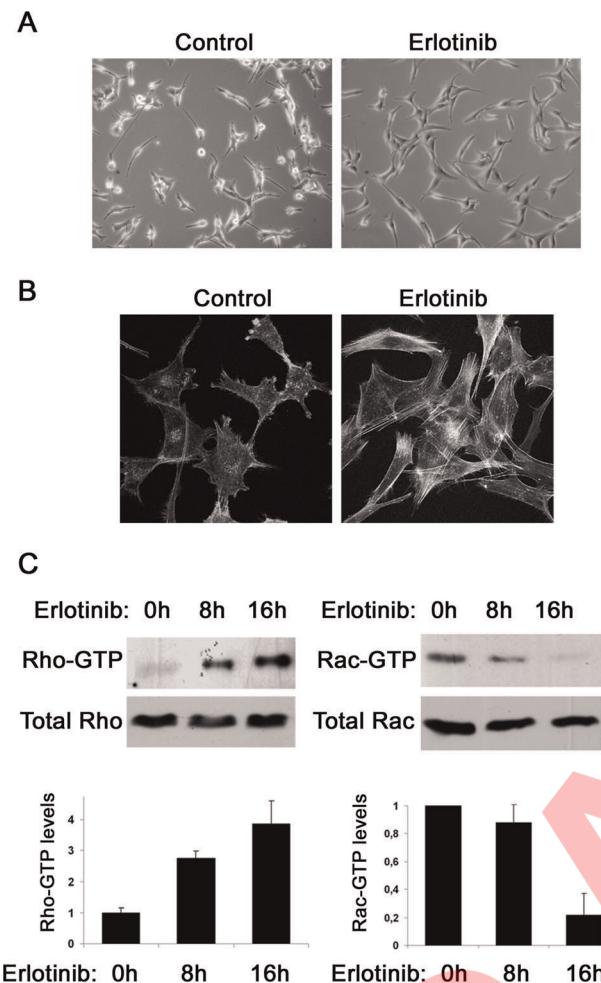
Figure 5. EGFR inhibition leads to actin cytoskeleton reorganization through Rho GTPase modulation. (A) Representative phase-contrast micrographs of U87MG cells left untreated (control) or treated for 24 h with 10 µM erlotinib (erlotinib). (B) U87MG cells grown on coverslips were left untreated (control) or were treated for 24 h with 10 µM erlotinib (erlotinib), fixed and stained with TRITC-labelled phalloidin. Bar, 5 µm. (C) U87MG cells were treated as indicated, harvested and RhoA and Rac1 activation were analyzed by GST-Rhotekin and GST-PBD pulldown, respectively, followed by western blotting with anti-RhoA and anti-Rac1 antibodies (upper panel). An aliquot of each lysate was also loaded in another gel to analyze total RhoA and total Rac1 levels (bottom panel). The graphs represent the quantified mean ± SD Rho/Rac activation values (Rho-GTP/Total Rho and Rac-GTP/Total Rac), relative to untreated cells, from three independent experiments.
doi:10.1371/journal.pone.0038770.g005

in three representative glioma cell lines (LN229, T98G and U373) with high, medium and low sensitivity to erlotinib. Erlotinib clearly inhibited both ERK and Akt phosphorylation in LN229 cells, which also showed a marked downregulation of cyclin D1 and a strong increase in $p27^{kip1}$ levels (Figure 4C). However, $p27^{kip1}$ levels did not increase in T98G cells, which show slightly lower sensitivity to erlotinib (Figure 4C). The behaviour of U373 cells, the least sensitive cell line, was different to that of LN229 and T98G cells. In U373 cells, erlotinib did not alter cyclin D1 levels nor Akt or ERK phosphorylation, although it induced $p27^{kip1}$ upregulation (Figure 4C). Interestingly, the sensitivity to erlotinib could not be correlated with the expression levels of EGFR (Figure 4A). Taken together, our results suggest that the inhibition

of signaling pathways converging on cell cycle regulatory elements mediate the antiproliferative effects of erlotinib in glioma cells.

EGFR inhibition leads to actin cytoskeleton reorganization and morphological changes in glioma cells perturbing Rho GTPase signaling

Our initial observations suggested that EGFR inhibition induced morphological changes in glioma cells (Figure 1A). We used U87MG cells to further investigate this alteration, since in these cells erlotinib exerted a robust effect on cell morphology. Untreated U87MG cells were relatively small, morphologically heterogeneous and loosely attached, with many cells eventually rounding up (Figure 5A). In contrast, erlotinib-treated U87MG cells were significantly larger, more homogeneous, firmly attached and well spread (Figure 5A). These results suggested that EGFR inhibition induced a profound cytoskeletal rearrangement. We thus evaluated the organization of the actin cytoskeleton in control and erlotinib-treated U87MG cells. F-actin staining indicated that polymerized actin was mostly located within the cell periphery in untreated U87MG cells, which were largely devoid of actin stress fibres (Figure 5B). Interestingly, erlotinib increased actomyosin contractility, as indicated by the assembly of actin stress fibres (Figure 5B). Since the dynamic regulation of the actin cytoskeleton is controlled by Rho GTPases [15], we monitored the activity of both Rho and Rac upon EGFR inhibition. Basal Rho activity is low in U87MG cells, but erlotinib induced a rapid and sustained activation of Rho, in agreement with the observed increase in actin stress fibres (Figure 5C). In sharp contrast, erlotinib dramatically reduced Rac activity in U87MG cells (Figure 5C). These results indicate that EGFR inhibition promotes the reorganization of the actin cytoskeleton through the modulation of Rho GTPase signaling.

Erlotinib inhibits glioma cell motility and invasion

Actin cytoskeleton reorganization in response to Rho GTPase signaling plays a crucial role in the regulation of cell motility [16]. We therefore investigated whether EGFR inhibition could also modulate glioma cell motility. For this purpose, we performed wound-healing assays in untreated and erlotinib-treated U87MG cells. Control U87MG cells were highly motile and migrated very efficiently in wound-healing assays (Figure 6A). Interestingly, erlotinib clearly inhibited cell motility in these assays (Figure 6A and 6B). Cell motility inhibition in response to erlotinib was also clearly observed in both T98G and LN229 cells (Figure 6A and 6B). Since increased motility and invasiveness are hallmarks of malignant glioma cells, we also tested whether EGFR inhibition could reduce glioma cell invasion in a 3D context. To this end, we monitored cell invasion using matrigel-coated transwells. In agreement with our previous data, whilst untreated glioma cells were highly invasive, cell invasion was strongly inhibited in erlotinib-treated cells (Figure 6C).

Erlotinib-induced effects on cell morphology and motility require Rho/ROCK activity

Our previous observations suggest that the increase in Rho activity and actomyosin contractility are responsible for the reduction in cell motility observed in response to EGFR inhibition. In order to confirm this hypothesis, we treated cells with erlotinib and tested whether Rho/ROCK inhibition could restore cell morphology and motility to similar conditions as those observed in untreated cells. As opposed to control cells, erlotinib-treated cells showed their distinctive morphology, characterized by the presence of larger, more homogeneous and firmly attached cells
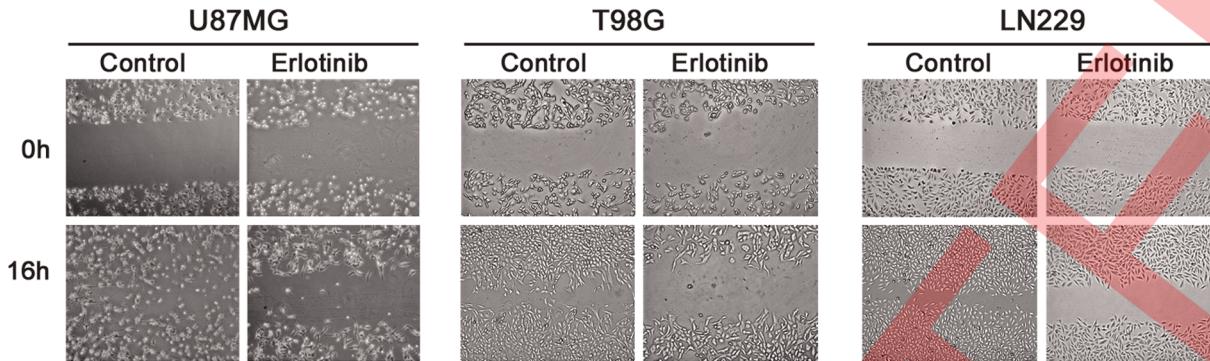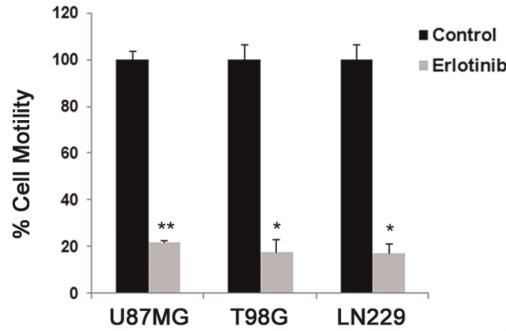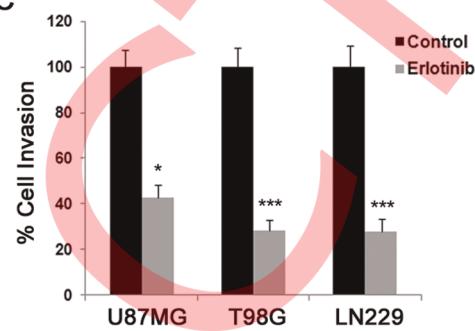
Figure 6. EGFR inhibition reduces glioma cell motility and invasion. (A) Representative phase-contrast micrographs of U87MG cells left untreated or treated with 10 μM erlotinib as indicated, before (upper panel) and after (lower panel) performing wound healing assays as described in Materials and Methods. (B) Representation of the mean ± SD rate of motility, from three independent experiments performed in sextuplicate, expressed as the percentage of U87MG cell motility relative to untreated cells. The differences between control and erlotinib treatment are statistically significant (Student's t-test: *P<0.05 and **P<0.01, respectively). (C) U87MG cells were seeded onto Matrigel-coated transwells in the absence (−) or presence (+) or 10 μM erlotinib to perform invasion assays as described in Materials and Methods. The graph represents the mean ± SD rate of invasion from three independent experiments performed in duplicate, expressed as the percentage of invasion relative to untreated cells. The differences between control and erlotinib treatment are statistically significant (Student's t-test: *P<0.05 and ***P<0.001, respectively).
doi:10.1371/journal.pone.0038770.g006

(Figure 7A). Interestingly, treatment of U87MG cells with either a Rho inhibitor (the C3 exoenzyme) or a small-molecule ROCK inhibitor (H-1152) together with erlotinib resulted in a very similar cellular morphology to that of control cells (Figure 7A). Accordingly, whereas erlotinib induced the formation of thick and robust stress fibres, co-treatment with either C3 or H-1152 completely prevented the formation of actin stress fibres (Figure 7B). We finally investigated whether Rho/ROCK inhibition could restore cell motility in erlotinib-treated glioma cells. To this end, we performed wound healing assays using U87MG cells in the presence of erlotinib alone or together with C3 or H-1152. In agreement with our previous data, EGFR inhibition led to a marked decrease in the rate of cell motility (Figure 7C). In sharp contrast, inhibition of either Rho or ROCK prevented erlotinib-induced reduction in cell motility, restoring the motility rate to that of untreated cells (Figure 7C). Rho/ROCK inhibitors also restored cell motility in erlotinib-treated T98G and LN229 cells (data not shown). Taken together, these results confirm that EGFR inhibitors alter glioma cell morphology and motility through the activation of the Rho/ROCK signaling pathway.

EGFR inhibition is effective in glioma cells with amplified or mutant EGFR

EGFR is frequently activated through mutation or amplification in malignant gliomas, although commonly-used glioma cell lines lack amplified or mutant EGFR. We therefore investigated whether EGFR inhibition was equally effective in the context of amplified or mutant EGFR. For this purpose we took advantage of the U87MG derivative cell line U87ΔEGFR, stably expressing the truncated and constitutively active EGFR mutant EGFRvIII [6,10], and the SKMG-3 cell line that maintains endogenous EGFR amplification and expresses high levels of wild-type EGFR [17]. Dose-response and growth curve experiments showed that both cell lines were sensitive to EGFR inhibition, similarly to the previously-characterized standard glioma cell lines (Figure 8A and 8B). In agreement with our previous data, EGFR inhibition also prevented multicellular tumour spheroid formation in U87ΔEGFR cells (Figure 8C). We next used multicellular tumour formation assays to investigate cooperation with TMZ. To this end, U87ΔEGFR cells were treated with sub-optimal doses of erlotinib (1–5 μM) and TMZ (25–50 μM), alone or in combination, and the formation of multicellular tumour spheroids was assessed. Similarly to untreated cells, cells treated with sub-optimal doses of erlotinib or TMZ alone gave rise to a high number of spheroids (Figure 8D). In contrast, the diverse combinations of sub-optimal doses of erlotinib and TMZ clearly reduced spheroid formation, similar to the standard erlotinib treatment (Figure 8D). We also investigated whether EGFR inhibition could reduce cell motility and invasion in the context of activated EGFR using wound-healing and transwell invasion assays, respectively. EGFR inhibition strongly reduced cell motility in both U87ΔEGFR and
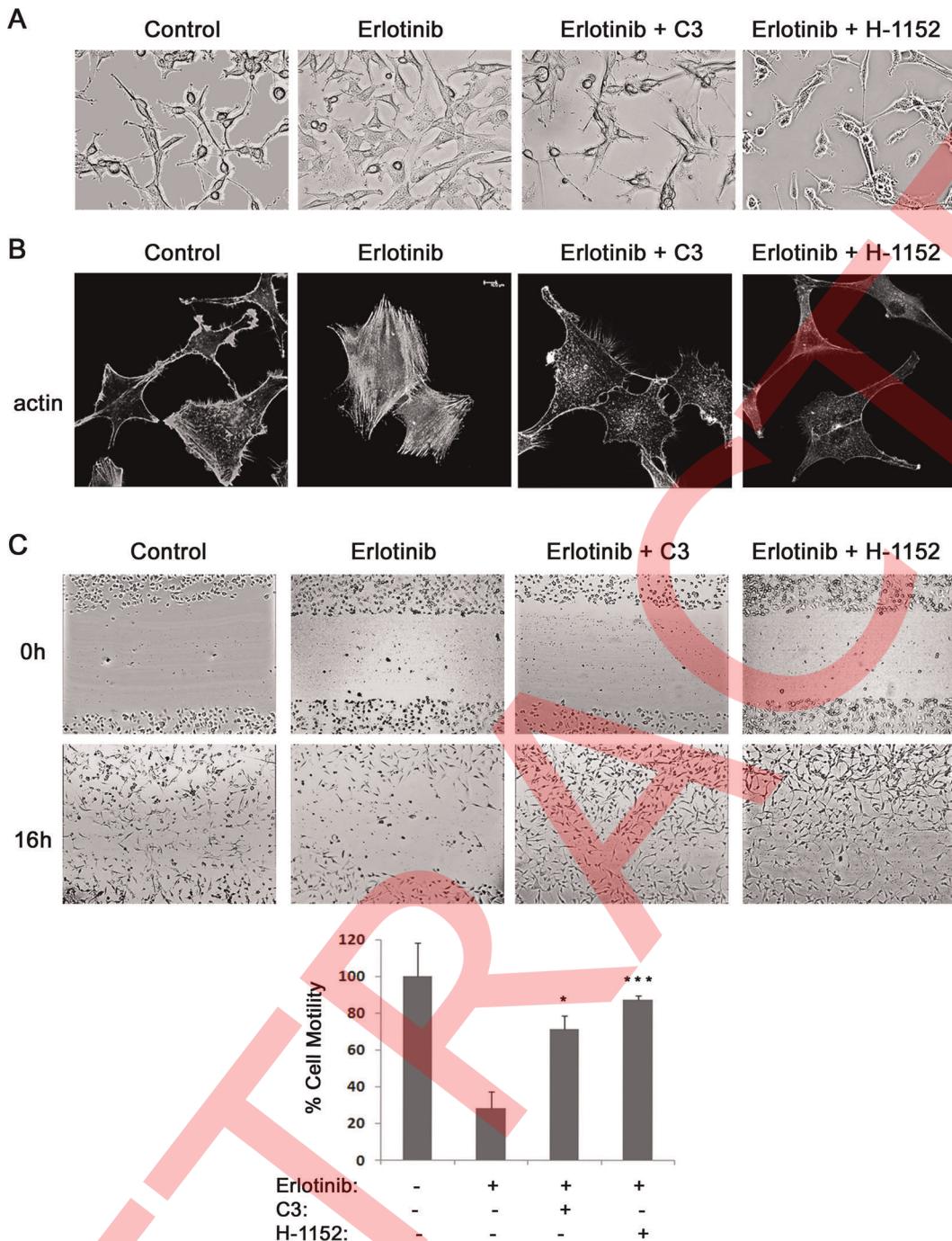
Figure 7. Erlotinib-induced effects on cell morphology and motility require Rho/ROCK activity. (A) Representative phase-contrast micrographs of U87MG cells left untreated (control) or treated for 24 h with 10 µM erlotinib alone or in the presence of 0,5 µg/ml C3 or 0,5 µM H-1152. (B) U87MG cells grown on coverslips were left untreated (control) or were treated for 24 h with 10 µM erlotinib alone or in the presence of 0,5 µg/ml C3 or 0,5 µM H-1152, fixed and stained with TRITC-labelled phalloidin. Bar, 10 µm. (C) Representative phase-contrast micrographs of U87MG cells left untreated or treated as indicated, before (upper panel) and after (lower panel) performing wound healing assays as described in Materials and Methods. The graph represents the mean ± SD rate of motility, from three independent experiments performed in sextuplicate, expressed as the percentage of U87MG cell motility relative to untreated cells. The differences in motility between cells treated alone with erlotinib or together with C3 or H-1152 are statistically significant (Student's t-test: *$P<0.05$ and ***$P<0.001$, respectively).
doi:10.1371/journal.pone.0038770.g007

SKMG-3 cells (Figures 8E and 8F) and this inhibitory effect on cell motility was significantly reverted by Rho/ROCK inhibitors C3 and H-1152 (data not shown). Cell invasion within a 3D matrix was also strongly inhibited in the presence of erlotinib in both cell lines (Figure 8G). Taken together, these results confirm that EGFR inhibition can effectively reduce glioma cell proliferation, motility and invasion in cells with enforced EGFR activation.
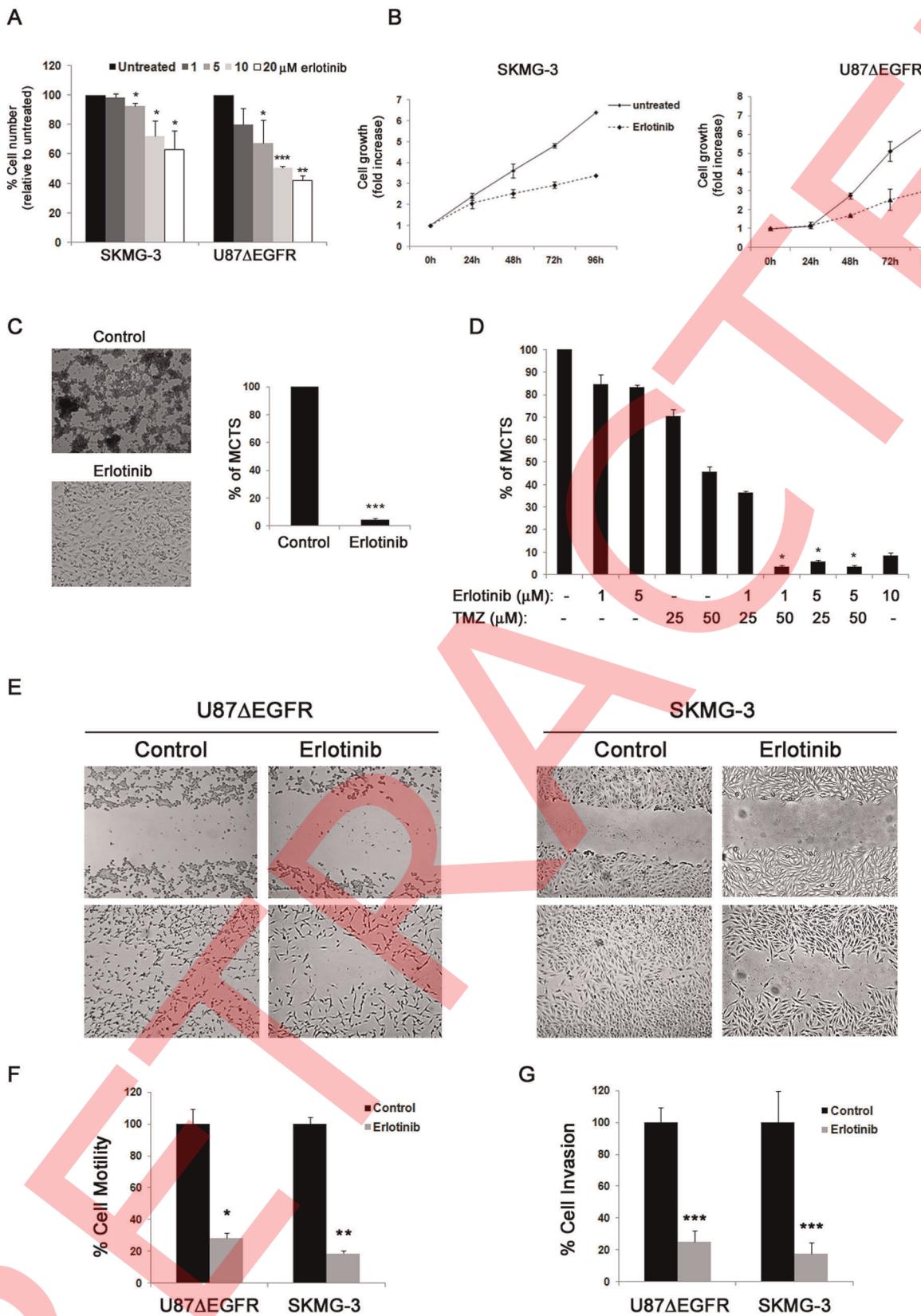
Figure 8. EGFR inhibition is effective in glioma cells with amplified or mutant EGFR. (A) SKMG-3 and U87ΔEGFR cells were treated for 72 h with the indicated concentrations of erlotinib. The mean ± SD values from three independent experiments, each conducted in duplicate, are shown in the graph, representing the percentage of viable cells relative to untreated conditions. The differences between control and erlotinib treatment are statistically significant (Student's t-test: *P<0.05, **P<0.01 and ***P<0.001, respectively). (B) SKMG-3 and U87ΔEGFR cells were left untreated (untreated) or treated with 10 μM erlotinib (erlotinib) and the number of cells counted every 24 h. The mean ± SD values from three independent

experiments, each conducted in duplicate, are shown in the graph, representing the fold increase in cell growth in untreated and erlotinib-treated conditions at the indicated time-points. (C) Representative phase-contrast micrographs of U87ΔEGFR cells left for 6 days to allow formation of multicellular tumour spheroids (MCTS), untreated (control) or treated with 10 µM erlotinib (erlotinib). The graph indicates the mean ± SD values of MCTS formation from three independent experiments, each conducted in duplicate, expressed as the percentage of MCTS relative to untreated cells. The differences between control and erlotinib treatment are statistically significant (Student's t-test: ***P<0.001). (D) U87ΔEGFR cells were left untreated or treated as indicated and grown for 6 days to allow formation of multicellular tumour spheroids (MCTS). The graph indicates the mean ± SD values of MCTS formation from three independent experiments, each conducted in duplicate, expressed as the percentage of MCTS relative to untreated cells. The differences between combined treatments and either treatment alone are statistically significant (Student's t-test: *P<0.05). (E) Representative phase-contrast micrographs of U87ΔEGFR (left panel) and SKMG-3 (right panel) cells left untreated or treated with 10 µM erlotinib as indicated, before (upper panel) and after (lower panel) performing wound healing assays as described in Materials and Methods. (F) Representation of the mean ± SD rate of motility, from three independent experiments performed in sextuplicate, expressed as the percentage of cell motility in each of the indicated conditions relative to untreated cells. The differences between control and erlotinib treatment are statistically significant (Student's t-test: *P<0.05 and **P<0.01, respectively). (G) U87ΔEGFR and SKMG-3 cells were seeded onto Matrigel-coated transwells in the absence or presence of 10 µM erlotinib to perform invasion assays as described in Materials and Methods. The graph represents the mean ± SD rate of invasion from three independent experiments performed in duplicate, expressed as the percentage of invasion relative to untreated cells. The differences between control and erlotinib treatment are statistically significant (Student's t-test: ***P<0.001).
doi:10.1371/journal.pone.0038770.g008

Discussion

In this report we have investigated the cellular effects of EGFR inhibition with erlotinib in a panel of human glioma cell lines. We consistently observed that erlotinib inhibited cell growth in all tested cell lines, leading to the accumulation of treated cells in G_1. A combination of dose-response and time-course growth assays indicated that 10 µM erlotinib inhibited glioma cell proliferation within a 30–80% range. Sensitivity to EGFR inhibition in cellular growth assays was strongly correlated with its ability to induce G_1 arrest, and was most apparent in LN229 and U87MG cells. A similar pattern of sensitivity to the EGFR inhibitor AG1478 has been recently reported [7]. We did not detect cellular death upon EGFR inhibition neither in cell viability nor in flow cytometry assays, in correlation with previous reports showing that EGFR inhibition mainly exerts cytostatic effects in glioma cells [6]. In agreement with its ability to inhibit glioma cell proliferation in culture, EGFR inhibition also suppressed the formation of multicellular tumour spheroids in U87MG cells. EGFR inhibition was equally effective in the context of amplified or mutated EGFR, since both SKMG-3 cells (with EGFR amplification and over-expression) [17] and U87ΔEGFR (stably expressing the truncated and constitutively active EGFRvIII) [6,10] were sensitive to erlotinib. Accordingly, EGFR inhibition also suppressed the formation of multicellular tumour spheroids in U87ΔEGFR cells.

Since the alkylating agent TMZ is routinely used in chemo-therapy to treat gliomas, we tested whether EGFR inhibition could cooperate with TMZ to prevent growth of glioma cells. We first used clonogenic assays to test whether inhibition of EGFR signaling sensitized glioma cells to TMZ-induced cytotoxicity. However, erlotinib pre-treatment had a protective effect against TMZ in this setting, probably related to accumulation of cells in G_1 induced by erlotinib and the consequent attenuation of the DNA damage elicited by TMZ, a hypothesis that was recently suggested [18]. Indeed, these results are in agreement with the observation that the efficacy of TMZ in glioma cells is cell cycle dependent, since E2F expression in glioma cells increases TMZ sensitivity, whereas p21^{cip1} expression reduces it [19]. We therefore assessed whether concomitant treatment with erlotinib and TMZ had any cooperative effects, although clonogenic assays could not be used for this purpose since the effects of TMZ are very robust and do not follow a linear dose-dependent pattern in these assays (data not shown). We thus performed MTT-based cell viability assays using low, sub-optimal, concentrations of both erlotinib and TMZ. In these conditions, concomitant treatment exerted a cooperative effect in both U251 and U87MG cells. Interestingly, concomitant treatment with sub-optimal concentra-tions of erlotinib and TMZ was able to synergistically suppress

multicellular tumour spheroid formation in both parental U87MG cells and their oncogenic, EGFRvIII-expressing, derivative U87ΔEGFR. Taken together, these data suggest that EGFR inhibitors can cooperate with TMZ for the treatment of gliomas, even at sub-optimal doses. However, our results also point out that drug scheduling is likely to influence the outcome of such treatments, and consequently should be taken into account in the design of clinical trials. In agreement with this, different scheduling regimens might be partially responsible for the conflicting data obtained in clinical trials with erlotinib in combination with TMZ in glioma patients. For instance, a phase I/II trial in which patients received treatment with erlotinib prior to its combination with TMZ and radiotherapy (RT) showed no benefit when compared to the standard historical treatment [20], whereas another clinical trial assessing a similar combination in which patients where administered erlotinib and TMZ continuosly from the beginning reported a better survival than historical controls [21]. Similarly, recent work in lung cancer cells has also highlighted the importance of drug scheduling when combining TKIs and conventional chemotherapeutic agents [22,23]. Note-worthy, the timing of administration in combinations of erlotinib or other TKIs leading to G_1 arrest together with radiotherapy in glioma patients should also be carefully considered, since cellular radiosensitivity has also been shown to be cell cycle dependent [24].

Our results do not support the notion that EGFR expression levels predict the response to EGFR inhibitors, in agreement with previous reports [5] and in contradiction with others [25]. Interestingly, it has been recently reported that small EGFR inhibitors such as AG1478, erlotinib, gefitinib and lapatinib, as opposed to the EGFR monoclonal antibody cetuximab, also reduce erbB3 and erbB4 phosphorylation, and this inhibition correlates with their cellular activity in glioma cells [7]. These observations raise the possibility that EGFR inhibitors might partially mediate their antitumoral effects through other members of the erbB family. Whatever the case, the cellular effects of EGFR inhibitors have been clearly associated with their ability to inhibit PI3K/Akt signaling and, accordingly, inhibitors of this pathway have been shown to potentiate the effects of EGFR inhibitors in sensitive cells and restore sensitivity in some resistant cell lines [10,11,26]. Not surprisingly, the most sensitive cell line in our panel, LN229, is the only one expressing wild type PTEN. Interestingly, our data indicate that PI3K/Akt inhibition is only apparent after several hours following EGFR inhibition, whilst ERK inhibition is an early event. This suggests that ERK inhibition is a direct consequence of EGFR receptor inhibition, probably through the inhibition of Ras/Raf signaling, whereas PI3K/Akt inhibition requires the suppression of further cellular

mediators, probably inhibiting their expression. For instance, long term EGFR inhibition could be required to inhibit the production of growth factors responsible for sustaining PI3K/Akt activity in the presence of EGFR inhibitors. Accordingly, it has been reported that combinatorial treatment with several receptor tyrosine kinase (RTK) inhibitors might be required to fully inhibit PI3K signaling in glioma cells [27]. The rapid and sustained inhibition of ERK phosphorylation observed in response to erlotinib could be used as a biomarker of appropriate drug delivery *in vivo* (i.e. to test whether the drug has reached the target), as opposed to a biomarker of drug efficacy, which fits clearly better with the monitoring of Akt phosphorylation, in agreement with the reported correlation between EGFR inhibitor sensitivity and Akt inhibition found in glioma cell lines [25] and glioma tumour-initiating cells (TICs) [28].

The sensitivity to erlotinib in different cell lines also correlated with changes in the expression of essential cell cycle modulators. A similar pattern of molecular changes has been reported in response to the EGFR inhibitor AG1478 [7]. EGFR inhibition induced cyclin D1 downregulation, which has been shown to be regulated at different levels downstream of both the Ras/Raf/MEK/ERK and the PI3K/Akt pathways [29–31]. In parallel, EGFR inhibitors increased $p27^{kip1}$ levels, which can also be regulated downstream of the PI3K/Akt pathway, for instance by FOXO-dependent transcription [32]. These changes in cyclin D1 and $p27^{kip1}$ levels are likely to be responsible for the inhibition of G_1 cyclin-dependent kinases regulating pocket protein phosphorylation and E2F release. Consequently, EGFR inhibition induced pRb hypophosphorylation in glioma cells, in correlation with the observed cell cycle arrest in G_1.

We also observed that EGFR inhibition in glioma cells induced dramatic morphological changes suggestive of actin cytoskeleton rearrangements. EGFR inhibition promoted the formation of robust actin stress fibres resulting in an increase in cellular spreading and attachment. Interestingly, such dramatic effects on cell morphology might be responsible, at least partially, of the strong inhibition of spheroid formation from U87MG monolayers elicited by erlotinib. Since these cytoskeletal alterations are under the control of Rho family GTPases [15,33], we investigated whether EGFR inhibitors could regulate Rho and Rac activity in glioma cells. Interestingly, erlotinib treatment inhibited Rac and concomitantly increased Rho activity levels. These results are in agreement with several studies reporting such an inverse functional crosstalk between Rho and Rac GTPases [34]. For example, Ras inhibition with S-trans, trans-farnesyl thiosalicylic acid (FTS) in glioma cells also reduces Rac activity whilst increasing Rho activation [35]. Indeed, EGFR inhibition might lead to Rho activation as a consequence of Rac inhibition, which is probably due to the inhibition in PI3K/Akt signaling. Interestingly, Rac expression has been associated with resistance to erlotinib in glioma cells [36], and the combination of EGFR inhibitors with statins, which perturb Rho GTPase membrane localization and function [37], synergize to inhibit glioma cell growth irrespective of EGFRvIII and PTEN status [38].

Crucially, the increase in Rho-dependent actomyosin contractility resulted in a significant inhibition in glioma cell motility. This is probably associated with an increased rigidness of erlotinib-treated cells, as a consequence of the Rho-mediated assembly of actin stress fibres, which also leads to focal adhesion formation and an increase in cell attachment [16]. Noteworthy, these effects are likely to be cell-type dependent, since the balance of active Rho and Rac dictates different outcomes in different cell types. Importantly, these effects on glioma cell morphology and motility were causally related to the increase in Rho/ROCK activity, since inhibition of either Rho or ROCK alone was sufficient to restore the organization of the actin cytoskeleton and the rate of cell motility to control conditions. Moreover, invasion of glioma cells within a three-dimensional matrix was also compromised in the presence of EGFR inhibitors. This reduction in glioma cell motility and invasion was also observed in cell lines with amplified or mutant EGFR. These results are relevant considering that tumour cell invasion is a biological feature of particular importance for the clinical outcome of gliomas [39]. Our data thus support the use of EGFR inhibitors to reduce the infiltration of glioma cells. For example, EGFR inhibitors could be useful to minimize local invasion prior to surgery. Alternatively, EGFR inhibition could be used in combination with radiotherapy, since irradiation has been shown to increase glioma invasiveness under some circumstances [40], and this increase has been associated with Rho GTPase activity [41]. It would also be interesting to assess the combinatorial effects of different RTK inhibitors on glioma cell morphology, motility and invasion, since such combinations have already shown more effectiveness reducing glioma cell proliferation [27].

In summary, we have shown that EGFR inhibition in glioma cells perturbs intracellular signaling networks including Rho family GTPases and the ERK and Akt pathways, reducing glioma cell proliferation, motility and invasion. Our data also indicate that EGFR inhibition can cooperate with the alkylating agent TMZ in a schedule-dependent manner to reduce glioma cell growth. The implications of these findings could help to improve the design and interpretation of future clinical trials with EGFR inhibitors in glioma patients.

Acknowledgments

Author Contributions

Conceived and designed the experiments: GR SF JR PV. Performed the experiments: GR ETM PV. Analyzed the data: GR ETM SF JR PV. Wrote the paper: PV.

References

1. Maher EA, Furnari FB, Bachoo RM, Rowitch DH, Louis DN, et al. (2001) Malignant glioma: genetics and biology of a grave matter. Genes Dev 15: 1311-1333.

2. Halatsch ME, Schmidt U, Behnke-Mursch J, Unterberg A, Wirtz CR (2006) Epidermal growth factor receptor inhibition for the treatment of glioblastoma multiforme and other malignant brain tumours. Cancer Treat Rev 32: 74-89.

3. Nishikawa R, Ji XD, Harmon RC, Lazar CS, Gill GN, et al. (1994) A mutant epidermal growth factor receptor common in human glioma confers enhanced tumorigenicity. Proc Natl Acad Sci U S A 91: 7727-7731.

4. Huang HS, Nagane M, Klingbeil CK, Lin H, Nishikawa R, et al. (1997) The enhanced tumorigenic activity of a mutant epidermal growth factor receptor common in human cancers is mediated by threshold levels of constitutive

tyrosine phosphorylation and unattenuated signaling. J Biol Chem 272: 2927-2935.

5. Halatsch ME, Gehrke EE, Vougioukas VI, Botefur IC, F AB, et al. (2004) Inverse correlation of epidermal growth factor receptor messenger RNA induction and suppression of anchorage-independent growth by OSI-774, an epidermal growth factor receptor tyrosine kinase inhibitor, in glioblastoma multiforme cell lines. J Neurosurg 100: 523-533.

6. Mellinghoff IK, Wang MY, Vivanco I, Haas-Kogan DA, Zhu S, et al. (2005) Molecular determinants of the response of glioblastomas to EGFR kinase inhibitors. N Engl J Med 353: 2012-2024.

7. Carrasco-Garcia E, Saceda M, Grasso S, Rocamora-Reverte L, Conde M, et al. (2011) Small tyrosine kinase inhibitors interrupt EGFR signaling by interacting with erbB3 and erbB4 in glioblastoma cell lines. Exp Cell Res 317: 1476-1489.

8. Brandes AA, Franceschi E, Tosoni A, Hegi ME, Stupp R (2008) Epidermal growth factor receptor inhibitors in neuro-oncology: hopes and disappointments. Clin Cancer Res 14: 957-960.

9. Haas-Kogan DA, Prados MD, Tihan T, Eberhard DA, Jelluma N, et al. (2005) Epidermal growth factor receptor, protein kinase B/Akt, and glioma response to erlotinib. J Natl Cancer Inst 97: 880-887.

10. Wang MY, Lu KV, Zhu S, Dia EQ, Vivanco I, et al. (2006) Mammalian target of rapamycin inhibition promotes response to epidermal growth factor receptor kinase inhibitors in PTEN-deficient and PTEN-intact glioblastoma cells. Cancer Res 66: 7864-7869.

11. Fan QW, Cheng CK, Nicolaides TP, Hackett CS, Knight ZA, et al. (2007) A dual phosphoinositide-3-kinase alpha/mTOR inhibitor cooperates with block-ade of epidermal growth factor receptor in PTEN-mutant glioma. Cancer Res 67: 7960-7965.

12. Ren XD, Schwartz MA (2000) Determination of GTP loading on Rho. Methods Enzymol 325: 264-272.

13. Bradford MM (1976) A rapid and sensitive method for the quantitation of microgram quantities of protein utilizing the principle of protein-dye binding. Anal Biochem 72: 248-254.

14. Kolchinsky A, Roninson IB (1997) Drug resistance conferred by MDR1 expression in spheroids formed by glioblastoma cell lines. Anticancer Res 17: 3321-3327.

15. Ridley AJ (2001) Rho family proteins: coordinating cell responses. Trends Cell Biol 11: 471-477.

16. Ridley AJ (2001) Rho GTPases and cell migration. J Cell Sci 114: 2713-2722.

17. Thomas C, Ely G, James CD, Jenkins R, Kastan M, et al. (2001) Glioblastoma-related gene mutations and over-expression of functional epidermal growth factor receptors in SKMG-3 glioma cells. Acta Neuropathol 101: 605-615.

18. Krakstad C, Chekenya M (2010) Survival signalling and apoptosis resistance in glioblastomas: opportunities for targeted therapeutics. Mol Cancer 9: 135.

19. Gomez-Manzano C, Lemoine MG, Hu M, He J, Mitlianga P, et al. (2001) Adenovirally-mediated transfer of E2F-1 potentiates chemosensitivity of human glioma cells to temozolomide and BCNU. Int J Oncol 19: 359-365.

20. Brown PD, Krishnan S, Sarkaria JN, Wu W, Jaeckle KA, et al. (2008) Phase I/II trial of erlotinib and temozolomide with radiation therapy in the treatment of newly diagnosed glioblastoma multiforme: North Central Cancer Treatment Group Study N0177. J Clin Oncol 26: 5603-5609.

21. Prados MD, Chang SM, Butowski N, DeBoer R, Parvataneni R, et al. (2009) Phase II study of erlotinib plus temozolomide during and after radiation therapy in patients with newly diagnosed glioblastoma multiforme or gliosarcoma. J Clin Oncol 27: 579-584.

22. Cheng H, An SJ, Zhang XC, Dong S, Zhang YF, et al. (2011) In vitro sequence-dependent synergism between paclitaxel and gefitinib in human lung cancer cell lines. Cancer Chemother Pharmacol 67: 637-646.

23. Pan F, Tian J, Zhang X, Zhang Y, Pan Y (2011) Synergistic interaction between sunitinib and docetaxel is sequence dependent in human non-small lung cancer with EGFR TKIs-resistant mutation. J Cancer Res Clin Oncol 137: 1397-1408.

24. Pawlik TM, Keyomarsi K (2004) Role of cell cycle in mediating sensitivity to radiotherapy. Int J Radiat Oncol Biol Phys 59: 928-942.

25. Haas-Kogan DA, Prados MD, Lamborn KR, Tihan T, Berger MS, et al. (2005) Biomarkers to predict response to epidermal growth factor receptor inhibitors. Cell Cycle 4: 1369-1372.

26. Fan QW, Specht KM, Zhang C, Goldenberg DD, Shokat KM, et al. (2003) Combinatorial efficacy achieved through two-point blockade within a signaling pathway-a chemical genetic approach. Cancer Res 63: 8930-8938.

27. Stommel JM, Kimmelman AC, Ying H, Nabioullin R, Ponugoti AH, et al. (2007) Coactivation of receptor tyrosine kinases affects the response of tumor cells to targeted therapies. Science 318: 287-290.

28. Griffero F, Daga A, Marubbi D, Capra MC, Melotti A, et al. (2009) Different response of human glioma tumor-initiating cells to EGFR kinase inhibitors. J Biol Chem.

29. Weber JD, Raben DM, Phillips PJ, Baldassare JJ (1997) Sustained activation of extracellular-signal-regulated kinase 1 (ERK1) is required for the continued expression of cyclin D1 in G1 phase. Biochem J 326 (Pt 1): 61-68.

30. Takuwa N, Fukui Y, Takuwa Y (1999) Cyclin D1 expression mediated by phosphatidylinositol 3-kinase through mTOR-p70(S6K)-independent signaling in growth factor-stimulated NIH 3T3 fibroblasts. Mol Cell Biol 19: 1346-1358.

31. Amanatullah DF, Zafonte BT, Albanese C, Fu M, Messiers C, et al. (2001) Ras regulation of cyclin D1 promoter. Methods Enzymol 333: 116-127.

32. Medema RH, Kops GJ, Bos JL, Burgering BM (2000) AFX-like Forkhead transcription factors mediate cell-cycle regulation by Ras and PKB through p27kip1. Nature 404: 782-787.

33. Ridley AJ, Hall A (1992) The small GTP-binding protein rho regulates the assembly of focal adhesions and actin stress fibers in response to growth factors. Cell 70: 389-399.

34. Sander EE, ten Klooster JP, van Delft S, van der Kammen RA, Collard JG (1999) Rac downregulates Rho activity: reciprocal balance between both GTPases determines cellular morphology and migratory behavior. J Cell Biol 147: 1009-1022.

35. Goldberg L, Kloog Y (2006) A Ras inhibitor tilts the balance between Rac and Rho and blocks phosphatidylinositol 3-kinase-dependent glioblastoma cell migration. Cancer Res 66: 11709-11717.

36. Halatsch ME, Low S, Mursch K, Hielscher T, Schmidt U, et al. (2009) Candidate genes for sensitivity and resistance of human glioblastoma multiforme cell lines to erlotinib. Laboratory investigation. J Neurosurg 111: 211-218.

37. Riganti C, Aldieri E, Doublier S, Bosia A, Ghigo D (2008) Statins-mediated inhibition of rho GTPases as a potential tool in anti-tumor therapy. Mini Rev Med Chem 8: 609-618.

38. Cemeus C, Zhao TT, Barrett GM, Lorimer IA, Dimitroulakos J (2008) Lovastatin enhances gefitinib activity in glioblastoma cells irrespective of EGFRvIII and PTEN status. J Neurooncol 90: 9-17.

39. Giese A, Bjerkvig R, Berens ME, Westphal M (2003) Cost of migration: invasion of malignant gliomas and implications for treatment. J Clin Oncol 21: 1624-1636.

40. Wild-Bode C, Weller M, Rimner A, Dichgans J, Wick W (2001) Sublethal irradiation promotes migration and invasiveness of glioma cells: implications for radiotherapy of human glioblastoma. Cancer Res 61: 2744-2750.

41. Zhai GG, Malhotra R, Delaney M, Latham D, Nestler U, et al. (2006) Radiation enhances the invasive potential of primary glioblastoma cells via activation of the Rho signaling pathway. J Neurooncol 76: 227-237.